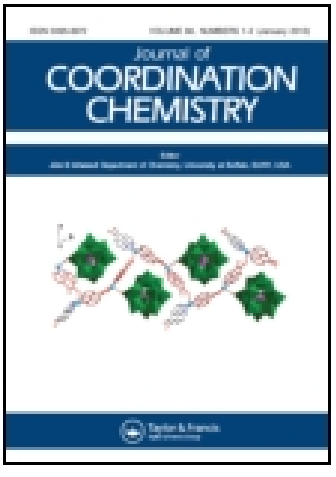

Journal of Coordination Chemistry
Publication details, including instructions for authors and subscription information:
http://www.tandfonline.com/loi/gcoo20

Counterion-induced modulation in biochemical properties of nitrile functionalized silver(I)-N-heterocyclic carbene complexes

Patrick O. Asekunowo[a] & Rosenani A. Haque[a]
[a] The School of Chemical Sciences, Universiti Sains Malaysia, Penang, Malaysia

Accepted author version posted online: 29 Sep 2014.Published online: 20 Oct 2014.

To cite this article: Patrick O. Asekunowo & Rosenani A. Haque (2014) Counterion-induced modulation in biochemical properties of nitrile functionalized silver(I)-N-heterocyclic carbene complexes, Journal of Coordination Chemistry, 67:22, 3649-3663, DOI: 10.1080/00958972.2014.971405

To link to this article: http://dx.doi.org/10.1080/00958972.2014.971405

Journal of Coordination Chemistry, 2014
Vol. 67, No. 22, 3649–3663, http://dx.doi.org/10.1080/00958972.2014.971405

Counterion-induced modulation in biochemical properties of nitrile functionalized silver(I)-*N*-heterocyclic carbene complexes

PATRICK O. ASEKUNOWO and ROSENANI A. HAQUE*

The School of Chemical Sciences, Universiti Sains Malaysia, Penang, Malaysia

(*Received 24 July 2014; accepted 11 September 2014*)

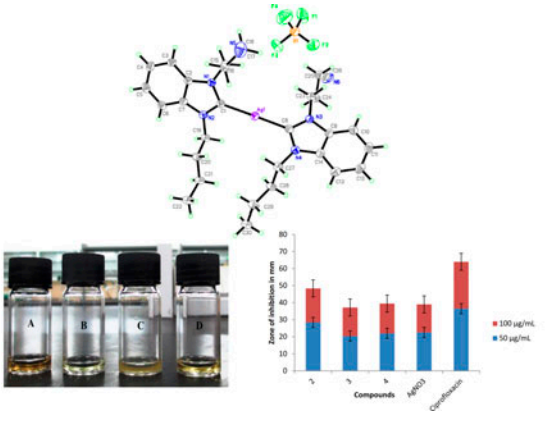

The new Ag(I) complexes (**2–4**) with proligand **1** were prepared and characterized as prospective antibacterial drug candidates. These compounds consist of a Ag(I) center linearly coordinated to two identical *N*-heterocyclic carbenes (NHCs). Crystal structures were solved for complexes **3** and **4**, the resulting structural data being in good agreement with expectations. We wondered whether the presence of different counter ions in these compounds might lead to modulation of their biological properties. Notably, in spite of their similar structural pattern, Ag(I)–NHC complex **2** with Br^- manifested better antibacterial actions than complexes **3** and **4** with PF_6^- and BF_4^-, respectively. Stability study over time in bacterial solutions revealed that these complexes have better stability than $AgNO_3$. Their interaction with DNA and RNA was explored, cleavage activity indicates that all Ag(I)–NHC complexes exhibited interesting nuclease activity via non-oxidative pathway.

Keywords: Ag(I)–NHC complex; Antibacterial activity; DNA cleavage; *N*-heterocyclic carbene; X-ray diffraction

*Corresponding author. Email: rosenani@usm.my

1. Introduction

The research community has shown considerable interest in the investigation of the antibacterial activity of silver, owing to the inability of bacteria to develop resistance toward silver ions [1, 2]. The efficacy of silver for domestic uses has been recognized for centuries, and silver containers have been used for ages in the purification of potable water, since Ag^+ is toxic to a broad range of microorganisms [3, 4]. In low concentrations, silver is not toxic for human cells, and hence it can be considered as an environmentally friendly antimicrobial. The antimicrobial activity of Ag is mainly due to its involvement with the electron transport system of the cell, its interference with the cell membrane and its interaction with the thiol groups of the vital enzymes of bacteria [5]. The slow release of Ag^+ at wound sites is vital for accelerated healing and preventing infections [6]. Therefore, the main challenge is to develop Ag-based antimicrobial agents that can facilitate the slow and constant release of Ag ions over a period of time in the affected area [7]. In this case, stable *N*-heterocyclic carbene (NHC) Ag(I) complexes have given promising results. This is attributed to their strong ability to bind to Ag [6–9]. This binding may result in more stable complexes that can slowly release Ag ions, such that the antimicrobial effect can be retained over a long period of time. Furthermore, the control over the electronic and steric properties of ligands is of critical importance for stabilizing a variety of transition metal complexes [10, 11]. Subtle variations of steric bulk and electron density at the active site may have drastic effects on the antibacterial properties [12, 13]. We have previously reported that increase in chain length at *N*-positions also increased the antibacterial activities [12, 13]. Therefore, **1**–**4** were synthesized to further investigate the effect of counter-anions on the antibacterial activity. However, studies in the literature that attempt to understand the mechanism of action of the counter-ion are scant. Emerging evidence has demonstrated that the counter ion is an extremely important aspect of pharmaceutical systems [14]. Studies done by Cetinkaya *et al.* [15] explored the effects of anions on the antimicrobial activity associated with a series of 1,3-diazolidinium salts. Variation of the counter-ion of the imidazolidinium salt greatly affected its antimicrobial activity. The mesitylmethyl derivative of the salts showed more effectiveness, especially with Cl^- than its counterparts such as PF_6^- and BF_4^-. This paper deals with the possible effects of three different anions, Br^-, PF_6^-, and BF_4^- on the antibacterial and nuclease activities of these new Ag(I)–NHC complexes.

2. Experimental

2.1. *Materials, methods, and instruments*

All chemicals were used as received. All solvents were redistilled except acetonitrile and dimethylsulfoxide, which were of AR grade. Benzimidazole, 1-bromobutane, 4-bromobutyronitrile, sodium tetrafluoroborate, potassium hexafluorophosphate, silver nitrate, and ciprofloxacin (standard used in antibacterial activity) were purchased from Sigma Aldrich. NMR spectra were recorded on a Bruker 500 MHz spectrometer at room temperature in DMSO-d_6 using TMS as an internal standard. FTIR spectra were recorded on a Perkin Elmer-2000 system spectrometer from 4000 to 400 cm^{-1}. Elemental analysis was carried out on a Perkin Elmer series II 2400 microanalyzer. Melting points were measured using a Stuart Scientific SMP-1 (UK) instrument. Conductivity measurements were obtained from a Jenway 470

Table 1. Crystal data and structure refinement details for **3** and **4**.

	3	**4**
Formula	$C_{30}H_{38}N_6AgF_6P$	$C_{30}H_{38}N_6AgF_4B$
Formula wt.	735.50	677.34
Crystal system	Monoclinic	Monoclinic
Space group	*P21/c*	*P21/c*
a (Å)	13.9043(4)	14.2058(3)
b (Å)	17.8590(5)	17.6959(3)
c (Å)	12.9198(4)	12.3183(2)
α (°)	90	90
β (°)	91.177(2)	92.761(1)
γ (°)	90	90
V (Å^3)	3207.53(16)	3093.03(10)
Z	4	4
ρ_{cal}/g cm^{-3}	1.523	1.455
Temperature	100 K	100 K
μ (mm^{-1})	0.744	0.706
Crystal size (mm)	0.14 × 0.21 × 0.54	0.23 × 0.24 × 0.36
θ range (°)	1.5–30.2	1.4–30.1
R (int)	0.040	0.032
F(0 0 0)	1504	1392
R, *WR2*, *S*	0.0443, 0.0880, 1.04	0.0353, 0.0911, 1.02

Conductivity/TDS Meter, with conductivity resolution of 0.01μS–1mS* and accuracy of ±0.5% ±2 digits. The X-ray single-crystal structure analysis was obtained using a Bruker Smart ApexII-2009 CCD area detector diffractometer. Crystals were mounted on fine glass fiber or metal pin using viscous hydrocarbon oil. Data were collected on a Bruker-Smart ApexII-2009 CCD diffractometer equipped with graphite monochromated Mo-Kα (λ = 0.71073) radiation. Data collection temperatures were maintained at 100 K using open flow N_2 cryostreams. Integration was carried out by SAINT using the APEX^{II} software [16]. Solutions were obtained by direct methods using SHELXS 97, followed by successive refinements using full-matrix least-squares method against F^2 using SHELXL 97 [17]. The program X-seed was used as a graphical SHELX interface [18]. Crystal data and refinement details for **3** and **4** are provided in table 1.

2.2. *Synthesis of 1-cyanopropyl-3-butylbenzimidazolium bromide (1)*

A mixture of benzimidazole (1.60 g, 13.50 mM) and KOH (1.14 g, 20.25 mM) in DMSO (20 mL) was stirred for 1 h at room temperature and 4-bromobutyronitrile (2.00 g, 13.50 mM) was then added dropwise. After 2 h the mixture was poured into water (300 mL) and extracted with chloroform (3 × 30 mL). The extract was filtered thrice through four plies of Whatman filter papers to get a clear solution of the desired compound. The solvent was evaporated under reduced pressure to collect a thick fluid. The compound formed, *N*-cyanopropylbenzimidazole (0.60 g, 3.40 mM), was added dropwise in a stirring solution of 1-bromobutane (0.46 g, 3.40 mM) in acetonitrile (30 mL) and refluxed for 20 h. The solvent was removed under reduced pressure to give 1-cyanopropyl-3-butylbenzimidazolium bromide (**1**) as a white solid. Yield: 0.50 g (67%). Melting point: 131–133 °C. ^{1}H NMR (500 MHz, DMSO-d$_6$, 298 K, δ ppm): 0.85 (t, *J* = 7.0 Hz, 3H, CH_3); 1.35 (m, 2H, **CH_2**–CH_3); 1.78 (m, 2H, **CH_2**–CH_2–CH_2); 2.40 (m, 2H, **CH_2**–CH_2–CN); 2.80 (t, *J* = 7.0 Hz, 2H, CH_2–CN); 4.35 (t, *J* = 7.0 Hz, 2H, N–**CH_2**–R); 4.70 (t, *J* = 7.0 Hz, 2H,

N–**CH$_2$**–CH$_2$–CH$_2$–CN); 7.65–7.78 (m, 2H, benzimidazolium-CH); 7.90–8.06 (m, 1H, benzimidazolium-CH); 8.10–8.18 (m, 1H, benzimidazolium-CH); 10.05 (s, 1H, NC*H*N). ^{13}C{^{1}H} NMR (125 MHz, DMSO-d$_6$, 298 K, δ ppm): 10.2 (CH$_3$); 22.5 (CH$_2$–CH$_3$); 23.8 (**CH$_2$**–CH$_3$); 30.9 (**CH$_2$**–CN); 40.0 (N–CH$_2$); 48.7 (N–**CH$_2$**–CH); 116.5 (CN); 118.3, 121.5, 127.1, 132.5 (benzimidazolium-C); 137.5 (benzimidazolium-C2′). FTIR (KBr disk) in cm^{-1}, ~3048 (C–H$_{ar}$); 2975 (C–H$_{aliph}$) 1498 (C=N). Anal. Calcd for C$_{15}$H$_{20}$N$_3$Br: C, 55.90; H, 6.21; N, 13.04. Found: C, 56.54; H, 6.26; N, 13.39.

2.3. *Synthesis of 1-cyanopropyl-3-butylbenzimidazolium-silver(I) bromide (2)*

A mixture of **1** (0.50 g, 1.55 mM) and Ag$_2$O (0.36 g, 1.55 mM) in dichloromethane (40 mL) was stirred at room temperature for 24 h and covered with aluminum foil to avoid light. The reaction mixture was filtered through Celite to remove unreacted silver and the solvent was removed under reduced pressure. The resulting colorless filtrate was concentrated to 5 mL under vacuum. A white solid was afforded by addition of 100 mL diethylether to the filtrate. The obtained solid was redissolved in methanol and 150 mL of diethyl ether was added to reprecipitate the solid (**2**), which was isolated by filtration and dried. Yield: 0.8 g (64%). Melting point: 192–194 °C. ^{1}H NMR (500 MHz, DMSO-d$_6$, 298 K, δ ppm): 0.85 (t, J = 7.0 Hz, 6H, 2 × CH$_3$); 1.35 (m, 4H, 2 × **CH$_2$**–CH$_3$) 1.78 (m, 4H, 2 × **CH$_2$**–CH$_2$–CH$_2$); 2.40 (m, 4H, 2 × **CH$_2$**–CH$_2$–CN); 2.80 (t, J = 7.0 Hz, 4H, 2 × CH$_2$–CN); 4.35 (t, J = 7.0 Hz, 4H, 2 × N–**CH$_2$**–R); 4.70 (t, J = 7.0 Hz, 4H, 2 × N–**CH$_2$**–CH$_2$–CH$_2$–CN); 7.60–7.65 (m, 4H, benzimidazolium-CH); 7.77–7.86 (m, 2H, benzimidazolium-CH); 8.00–8.05 (m, 2H, benzimidazolium-CH). ^{13}C{^{1}H} NMR (125 MHz, DMSO-d$_6$, 298 K, δ ppm): 10.2 (CH$_3$); 22.5 (CH$_2$–CH$_3$); 23.8 (**CH$_2$**–CH$_3$); 30.9 (**CH$_2$**–CN); 40.0 (N–CH$_2$); 48.7 (N–**CH$_2$**–CH); 116.5 (CN); 124.3, 127.5, 129.1, 132.5 (benzimidazolium-C). 188.0 (C2–Ag). FTIR (KBr disk) in cm^{-1}, ~3115 (C–H$_{ar}$); 2967 (C–H$_{aliph}$); 1499 (C=N); 2226 (C≡N). Anal. Calcd for C$_{30}$H$_{38}$N$_6$AgBr: C, 56.25; H, 5.94; N, 13.12. Found: C, 56.52; H, 6.35; N, 13.48.

2.4. *Synthesis of 1-cyanopropyl-3-butylbenzimidazolium-silver(I) hexafluorophosphate (3)*

Complex **3** was prepared according to the same procedure for **2** except that bromide was replaced with hexafluorophoshate, by metathesis using KPF$_6$ (1 equiv.) in methanol (20 mL). The mixture was stirred at room temperature for 3 h and allowed to stand overnight. Then the solvent was removed under reduced pressure and the resultant white powder was washed with distilled water (3 × 5 mL) to remove unreacted KPF$_6$, and air dried. The compound was further purified by acetonitrile/dichloromethane to give a crystalline solid. Single crystals suitable for X-ray were obtained by the slow diffusion of diethylether into acetonitrile solution containing the complex. Yield: 0.75 g (66%). Melting point: 197–199 °C. ^{1}H NMR (500 MHz, DMSO-d$_6$, 298 K, δ ppm): 0.85 (t, J = 7.0 Hz, 6H, 2 × CH$_3$); 1.35 (m, 4H, 2 × **CH$_2$**–CH$_3$); 1.78 (m, 4H, 2 × **CH$_2$**–CH$_2$–CH$_2$); 2.40 (m, 4H, 2 × **CH$_2$**–CH$_2$–CN); 2.80 (t, J = 7.0 Hz, 4H, 2 × CH$_2$–CN); 4.35 (t, J = 7.0 Hz, 4H, 2 × N–**CH$_2$**–R); 4.70 (t, J = 7.0 Hz, 4H, 2 × N–**CH$_2$**–CH$_2$–CH$_2$–CN); 7.60–7.65 (m, 4H, benzimidazolium-CH); 7.77–7.86 (m, 2H, benzimidazolium-CH); 8.00–8.05 (m, 2H, benzimidazolium-CH). ^{13}C{^{1}H} NMR (125 MHz, DMSO-d$_6$, 298 K, δ ppm): 10.2 (CH$_3$); 22.5 (CH$_2$–CH$_3$); 23.8 (**CH$_2$**–CH$_3$); 30.9 (**CH$_2$**–CN); 40.0 (N–CH$_2$); 48.7 (N–**CH$_2$**–CH); 116.5 (CN); 124.3, 127.5, 129.1, 132.5 (benzimidazolium-C). 188.0 (C2–Ag). FTIR (KBr disk) in cm^{-1}, ~3115

($C–H_{ar}$); 2967 ($C–H_{aliph}$); 1499 (C=N); 2226 (C≡N). Anal. Calcd for $C_{30}H_{38}N_6AgF_6P$: C, 49.05; H, 5.21; N, 11.42. Found: C, 49.32; H, 5.65; N, 11.78.

2.5. *Synthesis of 1-cyanopropyl-3-butylbenzimidazolium-silver(I) tetrafluoroborate (4)*

Complex **4** was prepared according to the same procedure for **3** except that bromide was replaced with tetrafluoroborate. Single crystals suitable for X-ray were obtained by the slow diffusion of diethylether into acetonitrile solution containing the complex. Yield: 0.9 g (70%). Melting point: 197–199 °C. ^{1}H NMR and FTIR data are analogous to that of **3**. Anal. Calcd for $C_{30}H_{38}N_6AgF_4B$: C, 53.18; H, 5.61; N, 12.41. Found: C, 53.52; H, 5.95; N, 12.78.

2.6. *Antibacterial studies*

The antibacterial activities of the compounds were investigated against a gram-negative bacterium (*Escherichia coli*; ATCC 25922) and a gram-positive bacterium (*Staphylococcus aureus*; ATCC 12600) bacteria. Stock solutions of all compounds were prepared using DMSO. Antibacterial tests were performed using the Kirby Beur disk diffusion method [19]. Single colonies of *E. coli* and *S. aureus* from fresh culture agar plates were, respectively, cultured in two bottles containing 5 mL of Luria-Bertani (LB) broth solution (Tryptone 10 g, yeast extract 5 g, NaCl 10 g L^{-1}) and incubated overnight at 37 °C. The turbidity of each culture was adjusted by comparing it to 0.5 McFarland standard, which is equal to 1.58×10^8 CFU/mL or 0.5 (OD_{600} reading). Single colonies were suspended in the LB broth with incubation over a period of 2–5 h until an appropriate optical density (OD = 0.6–0.8) at 600 nm was achieved. Using sterile cotton buds, each bacterial lawn culture was spread uniformly on different agar plates before placing the antimicrobial assay disks (5 mm) on the plate. Four disks were placed on the agar plate and 20 µL volumes of the compounds, $AgNO_3$ and ciprofloxacin were loaded on the disks with concentrations at 100 and 50 µg mL^{-1} in order to test the effect of different concentrations. The plates were incubated at 37 °C for 24 h, after which the zones of clearance were measured in mm and calculated as a mean of three replicates. The effectiveness of these compounds in relation to inhibition zone was compared to silver nitrate based on its established antimicrobial properties [20] and ciprofloxacin which were used as positive controls. The minimum inhibitory concentration (MIC) of each compound was determined based on the lowest concentration of the compounds that inhibited the growth of bacteria using the broth dilution method [21]. Single colonies of *S. aureus* and *E. coli* were isolated from agar plates and were grown in 5.0 mL LB broth. The solutions were incubated at 37 °C for 24 h in a shaking incubator at 180 rpm to yield bacterial solutions. Stock solutions of the compounds were prepared by dissolving each in DMSO to prepare stock concentrations at 50 mg mL^{-1}. Respectively from each stock solution, 2 µL of the compounds, $AgNO_3$ and ciprofloxacin were dissolved in 2 mL of the broth culture and used to prepare six serial dilutions of 100, 50, 25, 12.5, 6.25, and 3.125 µg mL^{-1}. Serial dilutions were done for each compound by transferring 1 mL (100 µg mL^{-1}) of the compound solution from the first tube to the second tube already containing 1 mL of nutrient broth. Next, 1 mL from tube 2 was again transferred into tube 3 and same was repeated for tubes 4, 5, and 6 to give concentrations of 100, 50, 25, 12.5, 6.25, and 3.125 µg mL^{-1}, respectively. Prepared bacteria solution (5 µL) was added to the dilution series on a daily basis for 7 days and the tubes were incubated at 37 °C for 16 h in a shaking incubator at 180 rpm. Bacteria growth was noted by turbidity of

the solution in the tubes and MIC was determined by the lowest concentration of the compounds that prevented visible growth.

2.7. *Gel electrophoresis*

The extent to which the newly synthesized salt and the Ag(I)–NHC complexes could function as chemical nucleases was examined using plasmid DNA and RNA, pTS414 as a target. The electrophoresis method was employed to study the efficiency of cleavage by the test compounds [22]. The extracted plasmid DNA and RNA, pTS414 (10 μg mL^{-1}) and 1 μL of the test compound (50 μg mL^{-1}) were mixed in 50 mM Tris–HCl buffer (pH 8.00). The contents were incubated for 8 h at 37 °C. Plasmid extraction was done using a plasmid purification kit (Intron biotechnology, Kyungki-Do Korea) without the addition of RNase in order to extract both RNA and DNA. The electrophoresis was performed using 0.8% agarose gel. For each sample 5 μL of the mixture along with standard marker was carefully loaded into the well. The voltage used was 90 V running on 0.5 × Tris–acetate EDTA buffer and the gel was stained with ethidium bromide solution (10 μg mL^{-1}) for 15 min. The gel was subsequently exposed to UV light and captured by a gel documentation system (FluorChem HD2; ProteinSimple, Santa Clara, CA). The nucleating ability of the synthesized benzimidazolium salt/Ag–NHC complexes (**1–4**) was determined by its efficiency in cleaving/degrading the plasmid DNA and RNA.

3. Results and discussion

3.1. *Synthesis and characterization*

Nitrile-functionalized benzimidazolium salt, **1** is accessible in two steps starting from deprotonation and subsequent reaction with 4-bromobutyronitrile as shown in scheme 1. Treatment of *N*-cyanopropylbenzimidazole with 1-bromobutane in acetonitrile at reflux affords the benzimidazolium salt **1** in good yield. Unsymmetrically substituted Ag(I)–NHC complexes **2–4** were synthesized according to the reported procedure [23] through the reaction of salt **1** with Ag_2O. NHC transition metal complexes are often prepared via reaction of an (benz)imidazolium salt with a basic metal source such as Ag_2O or $Pd(OAc)_2$ to afford the desired complex. Hence, the benzimidazolium salt **1** was treated with Ag_2O in dichloromethane at room temperature for 24 h under exclusion of light. The target mono-Ag(I)–NHC complex **2** was isolated in good yield by solvent removal under reduced pressure. Complex **2** was further converted to **3**, by replacing the bromide with hexafluorophoshate, by metathesis using KPF_6 (1 equiv.) in methanol (20 mL). The mixture was stirred at room temperature for 3 h and allowed to stand overnight. The same procedure was also used for the formation of **4**, except that hexafluorophosphate was replaced with tetrafluoroborate. The reactions involved in the formation of Ag(I)–NHC complexes **2–4** are shown in scheme 2. Both benzimidazolium salt and corresponding Ag(I)–NHC complexes are non-hygroscopic and readily soluble in common organic solvents such as methanol, ethanol, acetonitrile, DMF, and DMSO. Combination of elemental analysis and spectroscopic data show an agreement with the proposed structure of the compounds, which is further confirmed by data obtained by single-crystal X-ray diffraction. Single crystals of **3** and **4** were obtained by the slow vapor diffusion of diethylether into solution of acetonitrile containing the complexes. However for **2**, colorless blocks were obtained, which proved unsuitable for X-ray studies.

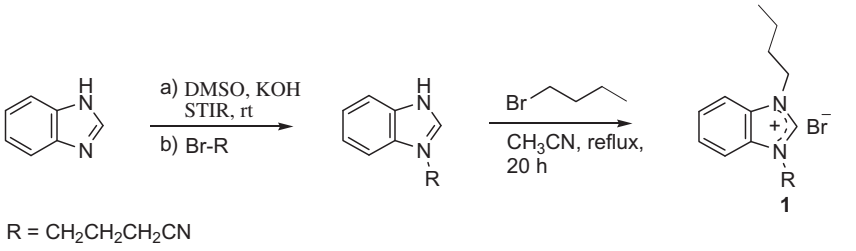

Scheme 1. Synthesis of the benzimidazolium salt (**1**).

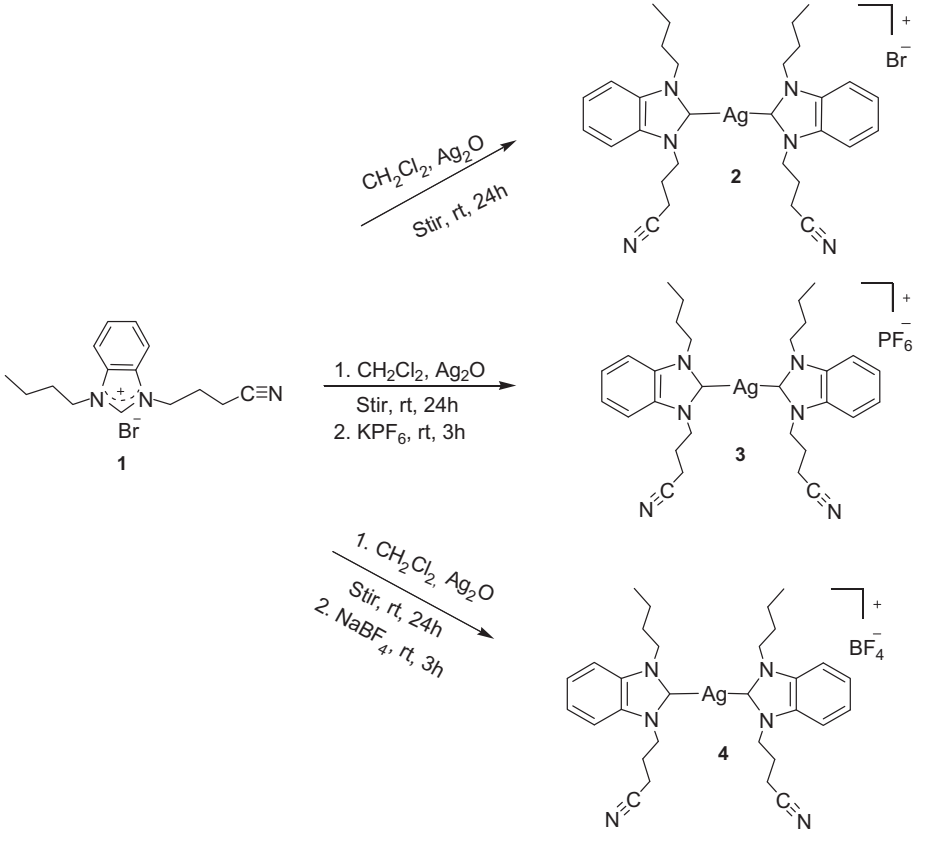

Scheme 2. Synthetic pathway to Ag(I)–NHC complexes (**2–4**).

3.2. *FTIR spectra of the compounds*

Relevant infrared frequencies along with their assignments for the proligand (**1**) and carbene complexes (**2–4**) are presented in the Experimental section. The spectra of **1** show a band of medium intensity at 3048–2975 cm^{-1}, which is assigned to ν(C–H, aliphatic and aromatic); it is present in all the carbene complexes with a shift of about 67 cm^{-1} for the

($C–H_{Ar}$). A sharp band at 2226 cm^{-1} is assigned to $\nu(C{\equiv}N)$ of the nitrile functionality in the proligand [24] and remains unchanged in the carbene complex spectra. This suggests the presence of nitrile functionality outside the coordination sphere and is because of the coordinatively saturated metal centers [25]. IR spectra of the proligand showed a band of medium intensity at 1498 cm^{-1}, which is assigned to benzimidazole ring ν(C=N) vibrations [26]. In the carbene complexes spectra, this band showed negligible shift (1499 cm^{-1}).

3.3. *NMR spectral studies*

NMR spectra of all compounds have been examined in suitable deuterated solvents over the scan ranges δ 0–16 and 0–200 ppm for ^1H and ^{13}C NMR spectral studies, respectively. The ^1H NMR spectrum of benzimidazolium salt shows multiplets at δ 7.65–8.18 and 1.35–2.40 ppm, due to aromatic and aliphatic protons. The spectrum also showed a characteristic downfield shift of NC*H*N signal of *N*-cyanopropylbenzimidazole from δ 8.17 to δ 10.05 ppm, suggesting the successful formation of the benzimidazolium salt **1** [27–29]. This downfield shift of the NC*H*N proton is due to deshielding by two adjacent electronegative nitrogens that withdraw electron density from around the benzimidazolium proton compared to other protons. The ^{13}C NMR spectrum of the benzimidazolium salt showed characteristic downfield resonance at ca. δ 137.5 ppm for the N*C*N carbon nuclei [30, 31]. In addition, spectrum also evidenced aromatic, nitrile, and aliphatic carbon resonances in the range δ 118.3–132.5, 116.5, and 10.2–48.7 ppm, respectively. The successful formation of carbene complexes is indicated by the absence of the characteristic acidic NC*H*N in the ^1H NMR spectra of **2–4** through deprotonation. Furthermore, in the ^{13}C NMR spectra of the complexes, the characteristic carbene carbon (C2–Ag) value at δ 180–188 ppm is observed. These observations collectively confirm the formation of desired Ag(I)–NHC complexes [32]. Apart from this major change, both ^1H and ^{13}C NMR spectra of the complexes showed resonances of aromatic, nitrile, and aliphatic carbon nuclei at δ 7.77–8.05, 0.85–4.70 ppm and 124.3–132.5, 116.5, 10.2–48.7 ppm, respectively. These values are in agreement with reported Ag(I)–NHC complexes [33–35].

3.4. *Molar conductivity measurements*

The molar conductance values of the benzimidazolium salt and complexes were obtained at room temperature in DMF at 10^{-3} M dm^{-3} concentration. The molar conductivity values of the benzimidazolium salt **1** and Ag(I)–NHC complex **2** are close, at 16.5 and 18.5 S cm^2 M^{-1}, while the values for **3** and **4** are 13.5 and 14.0 S cm^2 M^{-1}, respectively, indicating that they are 1 : 1 electrolytes [36]. However, **2** with the bromide counter ion was a relatively better electrolyte than **3** and **4** with different counter anions of PF_6^- and BF_4^-, respectively.

3.5. *Single-crystal X-ray diffraction studies*

Single crystals of these compounds suitable for X-ray diffraction analysis were obtained by slow diffusion of diethylether into a solution of the compound in methanol/acetonitrile at room temperature. Complex **3** crystallizes in the monoclinic space group *P21/c*, with one half of the molecule in the asymmetric unit (figure 1). The central Ag(I) has a linear coordination geometry through two carbene carbons (C1–Ag1–C8) with the bond angle of 178.19 (9)°. The two coordinated benzimidazolium rings are perpendicular to each other with a

dihedral angle of 45°. The molecule has a 'butterfly-like shape'. Both the nitrile entities point away from the metal center, showing their non-involvement in coordination. The bond distances of Ag1–C1 (2.096(2) Å) and internal bond angles at carbene carbon N1–C1–N2 (106.0(19)) are well within the range for a linear Ag(I)–NHC complex [12]. The planes of benzimidazole and nitrile group are almost perpendicular to each other. Both the nitrile substitutions are located on one side of the benzimidazole planes with *syn*-arrangement of the NHC ligands around the metal center. The hexafluorophosphates link the complex cations into 3-D networks through two different types of intermolecular C–H···F hydrogen bonds.

Complex **4** (figure 2) crystallized in the monoclinic space group *P21/c*. The Ag(I) of **4** is in a two-coordinate environment, which is best described as almost linear coordination geometry, with the carbene carbons of two NHC ligands. The Ag coordinates to two carbene groups with a distance of 2.087(2) Å for Ag1–C1. The C1–Ag1–C8 coordination angle of 179.2(8) is in agreement with those of similar silver(I)–NHC complexes [12, 37]. The planes of the benzimidazole ring are perpendicular to those of the other benzimidazole ring. This complex possesses one biscarbene complex cation and one tetrafluoroborate in the asymmetric unit. In the extended crystal structure, both complexes (**3** and **4**) showed similar intermolecular hydrogen bonds of C–H···F connecting the complex units into 3-D networks. Pertinent bond distances and angles of **3** and **4** are tabulated in table 2.

3.6. *Antibacterial activity*

Stock solutions of all compounds were prepared in DMSO. The concentrations of the test compounds were 3.125, 6.25, 12.5, 25, 50, and 100 μg mL^{-1} using silver nitrate for

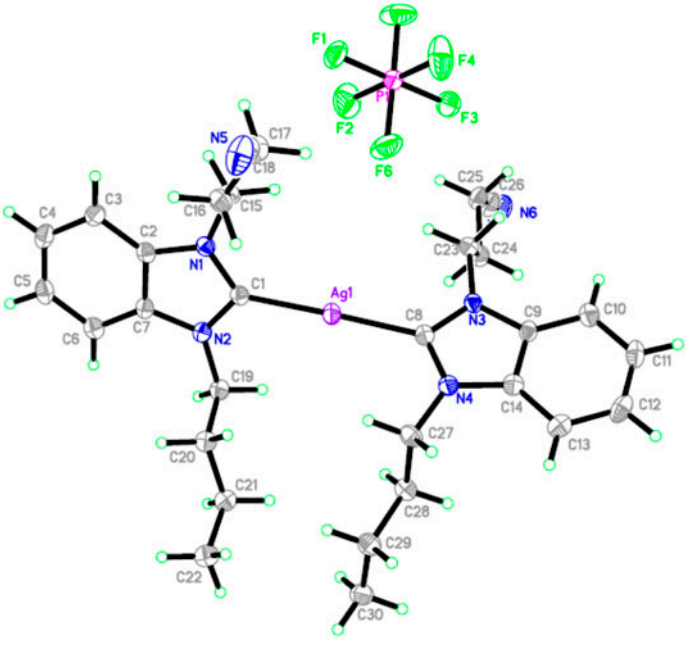

Figure 1. Structure of **3** with ellipsoids shown at 50% occupancies.

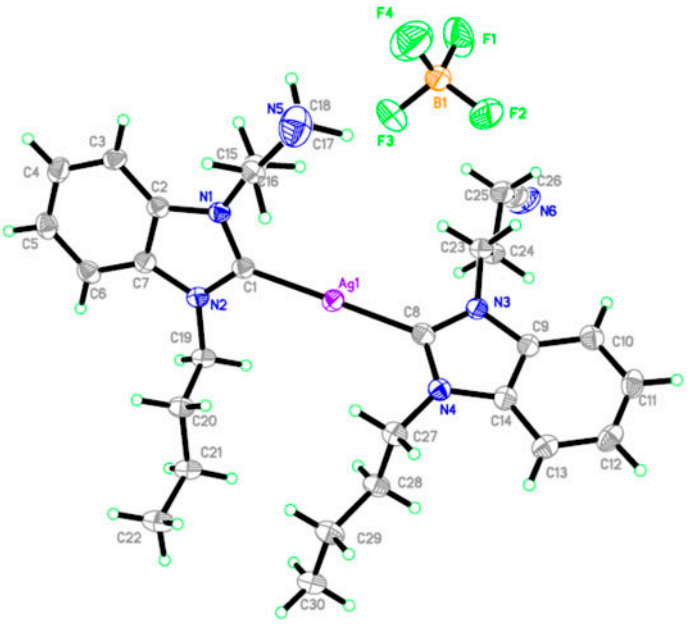

Figure 2. Structure of **4** with ellipsoids shown at 50% occupancies.

positive control and ciprofloxacin as the standard drug. In a solvent control test, the effect of 10% DMSO was studied on the growth of microorganisms, and no inhibitory activity was observed. To assess the stability of the complexes in the broth mixture, 10 mg mL^{-1} stock solutions of the complexes in DMSO were prepared and added in a 1 : 1 ratio to LB broth prepared in DMSO. This was done to imitate the conditions of the MIC evaluation experiments. The ^{1}H and ^{13}C NMR spectra were taken after 15 min and 48 h. The complexes demonstrated stability in the LB/DMSO broth mixture at 37 °C, as shown by the unchanged ^{1}H and ^{13}C NMR spectra after 48 h (see Supplementary material, figures S3 and S4, see online supplemental material at http://dx.doi.org/10.1080/00958972.2014.971405).

Compounds were screened for their antibacterial activities against *E. coli* and *S. aureus* using the disk diffusion method at concentrations of 50 and 100 μg mL^{-1}. The diameter of the inhibition zone was correlated with the susceptibility level of each microorganism against the test compound (table 3). In order to gain more quantitative data, broth dilution analysis was also performed in the present study (table 4). The MIC was determined based on the lowest concentration that inhibited the growth of the bacteria. The three counter

Table 2. Selected bond lengths [Å] and angles [°] for complexes 3 and 4.

	3	**4**
Ag1–C1	2.096(2)	2.087(2)
C1–N1	1.357(3)	1.356(3)
C1–N2	1.356(3)	1.391(3)
C1–Ag1–C8	178.2(9)	179.2(8)
N1–C1–N2	106.0(19)	106.2(17)

anions (Br^-, PF_6^-, and BF_4^-) on the complexes were replaced to explore the antibacterial potency. The two bacterial strains exhibited different susceptibilities to these compounds; the susceptibility levels of the gram-negative bacteria to the complexes were higher than those of the gram-positive bacteria. All complexes in this study were effective at inhibiting the growth of *E. coli* and *S. aureus* while their corresponding salt was inactive against both strains of bacteria. Complex **2** had higher inhibitory activity than **3** and **4**. The MIC values of the complexes against both *E. coli* and *S. aureus* are 12.5–50 μg mL^{-1} (table 4). Complex **2** (MIC, 12.5 μg mL^{-1}) possessing the bromide counter ions had significantly better antibacterial qualities than **3** and **4** bearing the hexafluorophosphate and tetrafluoroborate ions, respectively (MIC, 50 μg mL^{-1}). This could be due to better polarity of **2** compared to **3** and **4**, because there is need for medicinal agents to move through both aqueous and lipid media in the biological system. The relative solubility of a compound is a function of the presence of both lipophilic and hydrophilic features within the structures. Thus, the antibacterial effect could be due to fine tuning of the complexes based on the counter ions and substituents on the N-position in order to reach a compromise between the aqueous and lipid system. This will further facilitate the permeation of the complexes into the lipid layers which leads to blocking of the metal binding sites in the enzymes of microorganisms. The present result is in accord with our previous reports [38] where we mentioned that halide salts of compounds are more active than compounds with hexafluorophosphate as counter anions. These Ag–NHC complexes (**2–4**) bearing an electron-withdrawing nitrile functionality at N-position have superior stability over $AgNO_3$ in the bacterial solution since the growth of bacteria treated with these complexes on a daily basis were delayed for a longer time. The observed results can be explained by the slow decomposition of these Ag(I)–NHC complexes in the aqueous culture medium and the presence of electron-withdrawing nitrile group at the N-position. It was hypothesized that σ-withdrawers and π-donators led to reduction of σ-donor capability [39], thereby leaving the carbene carbon with less electron density and, therefore, less susceptible to attack by protons present in an aqueous environment. In all cases, the complexes have good-to-moderate bacteriostatic effect (MIC, 12.5–50 μg mL^{-1}) against both bacterial strains, especially **2** with MIC of 12.5 μg mL^{-1}.

During the last few years, a number of benzimidazole-based Ag(I)–NHC complexes were studied for their biological activity [40–44]. The present result reveals that the MIC values (12.5–50 μg mL^{-1}) of **2–4** are higher than those reported earlier I-III (chart 1) [41, 43, 44],

Table 3. Antibacterial activities of the compounds[a] against *E. coli* and *S. aureus* obtained by the disk diffusion method[b] (zone of inhibition ± SD/mm).

		Inhibition zone (mm)	
Test compound	Concentration in μg mL^{-1}	*E. coli*	*S. aureus*
2	50	19 ± 3	20 ± 1
3	50	16.3 ± 1.8	16.8 ± 0.5
4	50	16.6 ± 0.8	17.5 ± 1.5
$AgNO_3$	50	16.0 ± 0.5	16.5 ± 0.7
Ciprofloxacin	50	27.5 ± 0.5	25.5 ± 0.5
2	100	27.3 ± 1.8	28.4 ± 0.5
3	100	20 ± 8	20.5 ± 1.5
4	100	20.5 ± 1.8	22.0 ± 0.5
$AgNO_3$	100	22 ± 3	22.5 ± 1.7
Ciprofloxacin	100	35 ± 1	36 ± 3

[a]Compound **1** shows no activity.
[b]Test compound volume = 20 μL.

Table 4. MIC against *E. coli* and *S. aureus*.

Test compound	*E. coli* MIC ($\mu g\,mL^{-1}$)	*S. aureus* MIC ($\mu g\,mL^{-1}$)
2	12.5	12.5
3	50	25
4	50	25
$AgNO_3$	50	50
Ciprofloxacin	6.25	3.125

showing that these new Ag(I)–NHC complexes are quite potent. A marked dependence was noted on the nature of the counter-ion in the sense that changing the counter-ion on the complexes resulted in considerable differences in activity with respect to both gram-positive and gram-negative bacteria (table 3 and figure 3).

3.7. *Nuclease activity*

DNA cleavage is controlled by relaxation of supercoiled circular form of plasmid DNA into nicked circular form and linear form. When circular plasmid DNA is conducted by electrophoresis, the fastest migration will be observed for the supercoiled form (Form I). If one strand is cleaved, the supercoils will relax to produce a slower-moving open circular form (Form II). If both strands are cleaved, a linear form (Form III) will be generated that migrates in between [45]. The compounds can degrade the plasmid DNA and/or RNA [46]. Gel electrophoresis was used to evaluate the nuclease properties of **1**–**4**. Agarose gel image showing the nuclease activity of the compounds is shown in figure 4. Compounds **1**–**4** were studied for their nuclease activity by agarose gel electrophoresis against plasmid, pTS414 DNA/RNA in the absence of an oxidant. Plasmid extraction was done using a plasmid purification kit (Intron biotechnology, Kyungki-Do, Korea) without the addition of RNase in order to extract both RNA and DNA. pTS414 DNA/RNA was cultured, isolated, and used for the experiment. This method is intended to investigate the interaction of these synthesized compounds with DNA and/or RNA as an initial experiment to study likely mode of action(s) of the reported compounds. The electrophoresis analysis showed that the benzimidazolium salt **1** displayed no visible activity toward nucleic acids (lane 1); **2**, **3**, and **4** displayed distinct nuclease activity, as can be observed with their interaction with DNA [47]

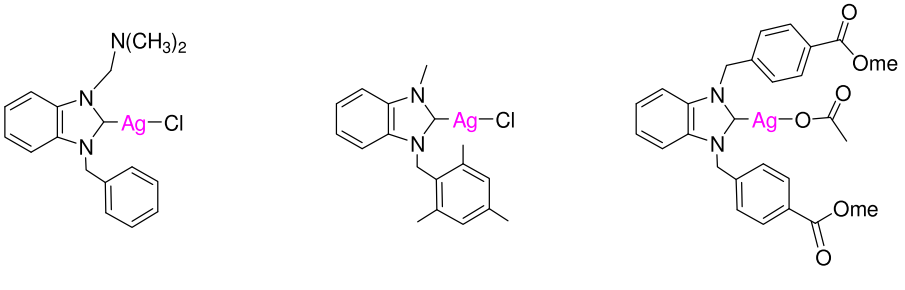

MIC = 50 μg/mL (I)

MIC = 100 μg/mL (II)

MIC = 59.5 μg/mL (III)

Chart 1. Previously reported benzimidazole-based-Ag(I)–NHC complexes with antibacterial activity.

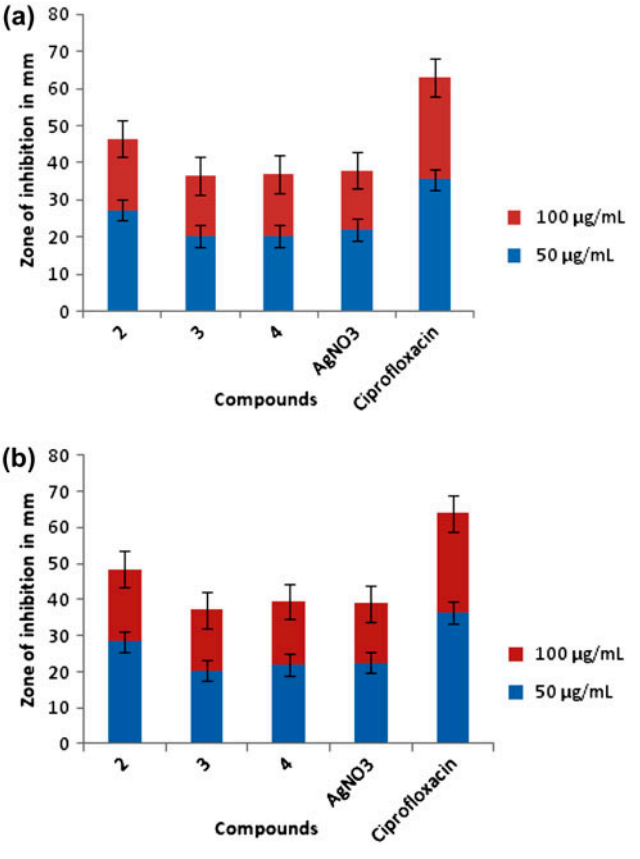

Figure 3. Antibacterial activities of the investigated compounds against (a) *E. coli* and (b) *S. aureus* at 50 and 100 µg mL^{-1}.

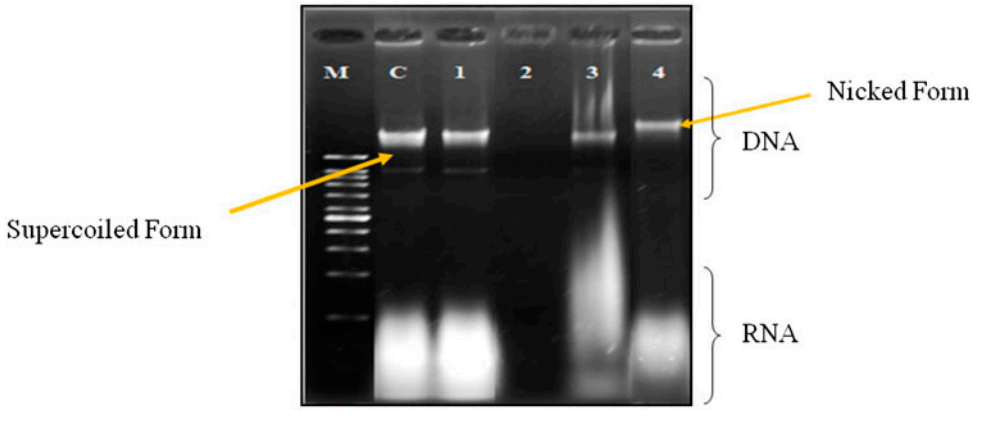

Figure 4. Nuclease activity (50 µg mL^{-1}); M = Marker; C = DNA/RNA alone; Lane 1-DNA/RNA + **1**; Lane 2-DNA/RNA + **2**; Lane 3-DNA/RNA + **3**; Lane 4-DNA/RNA + **4**.

and RNA in lanes 2, 3, and 4. Complex **2** clearly degraded the nucleic acids as can be seen in lane 2 showing complete disappearance of the associated bands on the gel [45]. Complexes **3** and **4** exhibited considerable DNA and RNA cleavage activity, with smearing in lane 3 revealing some degradation of the nucleic acids by **3**. Complex **4** converts supercoiled DNA (Form I) to the nicked form (Form II) and at the same time shows some degree of RNA degradation (lane 4). Figure 4 shows that the control DNA/RNA alone (C) does not show any apparent cleavage. This observation suggests that the complexes have potential to cleave nucleic acids by non-oxidative mechanism, possibly by hydrolytic path which remain to be clarified.

4. Conclusion

We have designed, formulated, and characterized a series of Ag(I)–NHC complexes (**2–4**) via reaction of benzimidazolium salt (**1**) with Ag_2O. Both benzimidazolium salt and the Ag(I)–NHC complexes were characterized by spectral and analytical methods. Complexes **3** and **4** were determined by crystal structures. Variation of the counter-ion of the complexes affected their antibacterial activities. The derivative with the Br^- (MIC, 12.5–25 $\mu g\,mL^{-1}$) was more effective than its PF_6^- and BF_4^- counterparts (MIC, 25–50 $\mu g\,mL^{-1}$) against both strains of bacteria. All the complexes exhibited interesting nuclease activity; **2** with the highest antibacterial activity also displayed the most efficient nuclease activity. This result provides some vital, yet preliminary insights into the mode of action that may control the observed antibacterial behavior of these complexes.

Supplementary material

Crystallographic data for the structure in this work has been deposited at the Cambridge Crystallographic Data Center, CCDC 1012942 and 1012943 Copies of these materials can be obtained from the Director, CCDC, 12 Union Road, Cambridge CB2 1EZ, UK (Fax: +44 1223 336033; E-mail: deposit@ccdc.cam.ac.uk.

Acknowledgements

R.A. Haque thanks Universiti Sains Malaysia for the Research University grant 1001/PKIMIA/811217. P.O. Asekunowo thanks IPS, USM for financial support [GA: PKD0004/12(R)].

References

[1] K.M. Hindi, M.J. Panzner, C.A. Tessier, C.L. Cannon, W.J. Youngs. *Chem. Rev.*, **109**, 3859 (2009).
[2] A. Melaiye, R.S. Simons, A. Milsted, F. Pingitore, C. Wesdemiotis, C.A. Tessier, W.J. Youngs. *J. Med. Chem.*, **47**, 973 (2004).
[3] D. Bourissou, O. Guerret, F.P. Gabbaï, G. Bertrand. *Chem. Rev.*, **100**, 39 (2000).
[4] J.C. Garrison, W.J. Youngs. *Chem. Rev.*, **105**, 3978 (2005).
[5] N.C. Kasuga, A. Sugie, K. Nomiya. *Dalton Trans.*, **21**, 3732 (2004).

[6] A.K. Kascatan-Nebioglu, M.J. Panzner, C.A. Tessier, C.L. Cannon, W.J. Youngs. *Coord. Chem. Rev.*, **251**, 884 (2007).
[7] S. Ray, R. Mohan, J.K. Singh, M.K. Samantaray, M.M. Shaikh, D. Panda, P. Ghosh. *J. Am. Chem. Soc.*, **129**, 15042 (2007).
[8] A. Melaiye, R.S. Simons, A. Milsted, F. Pingitore, C. Wesdemiotis, C.A. Tessier, W.J. Youngs. *J. Med. Chem.*, **47**, 973 (2004).
[9] K.M. Hindi, A.J. Ditto, M.J. Panzner, D.A. Medvetz, D.S. Han, C.E. Hovis, J.K. Hilliard, J.B. Taylor, Y.H. Yun, C.L. Cannon, W.J. Youngs. *Biomaterials*, **30**, 3771 (2009).
[10] A. John, P. Ghosh. *Dalton Trans.*, **39**, 7183 (2010).
[11] C. Dash, M.M. Shaikh, P. Ghosh. *J. Chem. Sci.*, **123**, 97 (2011).
[12] R.A. Haque, P.O. Asekunowo, M. Razali, F. Mohamad. *Heteroat. Chem.*, **25**, 194 (2014).
[13] R.A. Haque, P.O. Asekunowo, M. Razali. *J. Coord. Chem.*, **67**, 2131 (2014).
[14] A.T.M. Serajuddin. *Adv. Drug Deliv. Rev.*, **59**, 603 (2007).
[15] E. Çetinkaya, A. Denizci, I. Özdemir, H.T. Öztürk, I. Karaboz, B.J. Çetinkaya. *J. Chemother.*, **14**, 241 (2002).
[16] ApexII. *V2.1.0*, Bruker AXS, Madison, WI (2005).
[17] G.M. Sheldrick. *Acta Crystallogr. Sect. A*, **64**, 112 (2008).
[18] L.J. Barbour. *J. Supramol. Chem.*, **1**, 189 (2001).
[19] W.L. Drew, A.L. Barry, R. O'Toole, J.C. Sherris. *Appl. Microbiol.*, **24**, 240 (1972).
[20] A.B. Lansdown, A. Williams, S. Chandler, S. Benfield. *J. Wound Care*, **14**, 155 (2005).
[21] I. Wiegand, K. Hilpert, R.E.W. Hancock. *Nat. Protoc.*, **3**, 163 (2008).
[22] N. Raman, R. Jeyamurugan, A. Sakthivel, L. Mitu. *Spectrochim. Acta, Part A*, **75**, 88 (2010).
[23] H.M.J. Wang, C.Y.L. Chen, I.J.B. Lin. *Organometallics*, **18**, 1216 (1999).
[24] W.N.O. Wylie, A.J. Lough, R.H. Morris. *Organometallics*, **29**, 570 (2010).
[25] Q.-X. Liu, H.-L. Li, X.-J. Zhao, S.-S. Ge, M.-C. Shi, G. Shen, Y. Zang, X.-G. Wang. *Inorg. Chim. Acta*, **376**, 437 (2011).
[26] S. Budagumpi, V.K. Revankar. *Transition Met. Chem.*, **35**, 649 (2010).
[27] İsmail Özdemir, H. Arslan, S. Demir, D. VanDerveer, B. Çetinkaya. *Inorg. Chem. Commun.*, **11**, 1462 (2008).
[28] F. Li, J.J. Hu, L.L. Koh, T.S. Hor. *Dalton Trans.*, **39**, 5231 (2010).
[29] A.R. Chianese, X. Li, M.C. Janzen, J.W. Faller, R.H. Crabtree. *Organometallics*, **22**, 1663 (2003).
[30] T. Ramnial, C.D. Abernethy, M.D. Spicer, I.D. McKenzie, I.D. Gay, J.A.C. Clyburne. *Inorg. Chem.*, **42**, 1391 (2003).
[31] B.E. Ketz, A.P. Cole, R.M. Waymouth. *Organometallics*, **23**, 2835 (2004).
[32] R.A. Haque, A.W. Salman, T.S. Guan, H.H. Abdallah. *J. Organomet. Chem.*, **696**, 3507 (2011).
[33] V.J. Catalano, M.A. Malwitz. *Inorg. Chem.*, **42**, 5483 (2003).
[34] U.M. Tripathi, A. Bauer, H. Schmidbaur. *J. Chem. Soc., Dalton Trans.*, 2865 (1997).
[35] J.C.C. Chen, I.J.B. Lin. *Organometallics*, **19**, 5113 (2009).
[36] W.J. Geary. *Coord. Chem. Rev.*, **7**, 81 (1971).
[37] P. de Frémont, N.M. Scott, E.D. Stevens, T. Ramnial, O.C. Lightbody, C.L.B. Macdonald, J.A.C. Clyburne, C.D. Abernethy, S.P. Nolan. *Organometallics*, **24**, 6301 (2005).
[38] R.A. Haque, M.A. Iqbal, P. Asekunowo, A.A.M.S. Majid, M.B. Khadeer Ahamed, M.I. Umar, S.S. Al-Rawi, F.R.S. Al-Suede. *Med. Chem. Res.*, **22**, 1663 (2013).
[39] Q.L. Zhang, J.G. Liu, J.Z. Liu, H. Li, Y. Yang, H. Xu, H. Chao, L.N. Ji. *Inorg. Chim. Acta*, **34**, 339 (2002).
[40] R.A. Haque, N. Hasanudin, M.A. Iqbal, A. Ahmad, S. Hashim, A. Abdul Majid, M.B.K. Ahamed. *J. Coord. Chem.*, **66**, 3211 (2013).
[41] B. Yığıt, Y. Gök, İ. Özdemır, S. Günal. *J. Coord. Chem.*, **65**, 371 (2012).
[42] R.A. Haque, N. Hasanudin, M.A. Iqbal, A. Ahmad, S. Hashim, A. Abdul Majid, M.B.K. Ahamed. *J. Coord. Chem.*, **66**, 3211 (2013).
[43] S. Patil, K. Dietrich, A. Deally, B. Gleeson, H. Müller-Bunz, F. Paradisi, M. Tacke. *Helv. Chim. Acta*, **93**, 2347 (2010).
[44] İlknur Özdemir, S. Demir, S. Günal, İ. Özdemir, C. Arıcı, D. Ülkü. *Inorg. Chim. Acta*, **363**, 3803 (2010).
[45] Q.L. Zhang, J.G. Liu, J.Z. Liu, H. Li, Y. Yang, H. Xu, H. Chao, L.N. Ji. *Inorg. Chim. Acta*, **339**, 34 (2002).
[46] N. Raman, T. Baskaran, A. Selva. *J. Iran. Chem. Res.*, **1**, 29 (2008).
[47] H. Wu, Y. Zhang, H. Wang, Y. Bai, F. Shi, X. Wang, Z. Yang. *J. Coord. Chem.*, **67**, 1771 (2014).